Comprehensive Determination of Protein Tyrosine pK(a) Values for Photoactive Yellow Protein Using Indirect C-13 NMR Spectroscopy

Oktaviani, Nur Alia; Pool, Trijntje J.; Kamikubo, Hironari; Slager, Jelle; Scheek, Ruud M.; Kataoka, Mikio; Mulder, Frans A. A.

Published in:
Biophysical Journal

DOI:
10.1016/j.bpj.2011.12.024

Publication date:
2012

Comprehensive Determination of Protein Tyrosine pK_a Values for Photoactive Yellow Protein Using Indirect ^{13}C NMR Spectroscopy

Nur Alia Oktaviani,[†△] Trijntje J. Pool,[†△] Hironari Kamikubo,[‡] Jelle Slager,[†] Ruud M. Scheek,[†] Mikio Kataoka,[‡] and Frans A. A. Mulder[†*]

[†]Groningen Biomolecular Sciences and Biotechnology Institute, University of Groningen, Groningen, The Netherlands; and [‡]Graduate School of Materials Science, Nara Institute of Science and Technology, Nara, Japan

ABSTRACT Upon blue-light irradiation, the bacterium *Halorhodospira halophila* is able to modulate the activity of its flagellar motor and thereby evade potentially harmful UV radiation. The 14 kDa soluble cytosolic photoactive yellow protein (PYP) is believed to be the primary mediator of this photophobic response, and yields a UV/Vis absorption spectrum that closely matches the bacterium's motility spectrum. In the electronic ground state, the *para*-coumaric acid (*p*CA) chromophore of PYP is negatively charged and forms two short hydrogen bonds to the side chains of Glu-46 and Tyr-42. The resulting acid triad is central to the marked pH dependence of the optical-absorption relaxation kinetics of PYP. Here, we describe an NMR approach to sequence-specifically follow all tyrosine side-chain protonation states in PYP from pH 3.41 to 11.24. The indirect observation of the nonprotonated $^{13}C_\gamma$ resonances in sensitive and well-resolved two-dimensional ^{13}C-^{1}H spectra proved to be pivotal in this effort, as observation of other ring-system resonances was hampered by spectral congestion and line-broadening due to ring flips. We observe three classes of tyrosine residues in PYP that exhibit very different pK_a values depending on whether the phenolic side chain is solvent-exposed, buried, or hydrogen-bonded. In particular, our data show that Tyr-42 remains fully protonated in the pH range of 3.41–11.24, and that pH-induced changes observed in the photocycle kinetics of PYP cannot be caused by changes in the charge state of Tyr-42. It is therefore very unlikely that the *p*CA chromophore undergoes changes in its electrostatic interactions in the electronic ground state.

INTRODUCTION

Photoactive yellow protein (PYP) is a soluble, cytosolic protein from the purple phototropic eubacterium *Halorhodospira halophila*. PYP shows a UV absorption spectrum that closely matches the wavelength dependence of the escape of the bacterium from potentially harmful blue-light radiation (1). Consequently, PYP has become an important example of a soluble bacterial light sensor, and a rich model system for the study of PER-ARNT-SIM (PAS) domain signaling (2).

PYP consists of 125 residues that form a six-stranded β-sheet flanked by five α-helices in an α/β fold (3). In the active site, the *para*-coumaric acid (*p*CA) chromophore forms a thioester bond to the side chain of C69. This chromophore is stabilized by the formation of two short hydrogen bonds (H-bonds) between *p*CA and E46, and between *p*CA and Y42 (4,5), as shown in Fig. 1.

Recent high-resolution neutron and x-ray crystallographic structures reveal a shared low-barrier H-bond between *p*CA and E46, whereas the H-bond between *p*CA and Y42 is qualified as a short ionic H-bond (6). Sigala et al. (7) detected the two H-bonds using one-dimensional (1D) ^{1}H NMR. As depicted in Fig. 1, the phenolic oxygen of Y42 also participates as a proton acceptor in the H-bond formation with the hydroxyl proton of T50. Y94 is also involved in the H-bond network in the active center by donating its side-chain proton to the backbone oxygen of C69 (4,8).

Upon blue-light irradiation, PYP undergoes a number of changes in its optical properties that are associated with changes in its structure (9–11). Initially, the *p*CA chromophore undergoes a series of rapid bond isomerizations on the picosecond timescale to the pR state. This process is followed by proton transfer on the microsecond timescale, which involves the dissolution of the shared low-barrier H-bond (6) and protonation of *p*CA to form the pB′ state (12,13). Spectroscopic evidence has shown that the N-terminal domain of PYP dissociates from its PAS domain and becomes unfolded. This state is then recognized as pB, in which λ_{max} of the chromophore absorption changes from 446 nm (in the ground state, pG) to 355 nm (in the pB state) (14,15). Finally, the intermediate (pB) relaxes slowly (subsecond) to the initial pR state, a process that is associated with formation of the central β-sheet and part of the helical structures, and is succeeded by a consolidation of structure around the *p*CA chromophore (14). The

Submitted September 2, 2011, and accepted for publication December 5, 2011.

△Nur Alia Oktaviani and Trijntje J. Pool contributed equally to this work.

*Correspondence: f.a.a.mulder@rug.nl

Frans A.A. Mulder's present address is Interdisciplinary Nanoscience Center (iNANO) and Department of Chemistry, University of Aarhus, Aarhus, Denmark.

Editor: Bertrand Garcia-Moreno.

0006-3495/12/02/0579/8

doi: 10.1016/j.bpj.2011.12.024

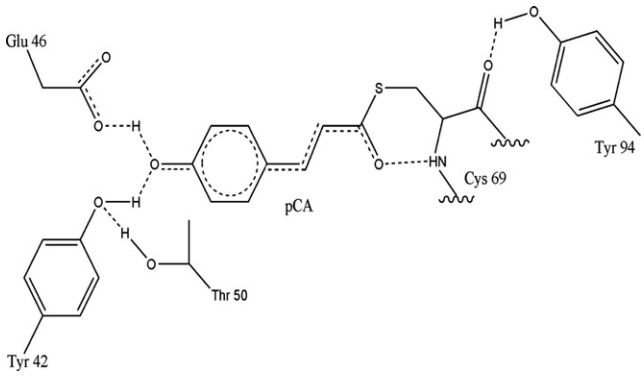

FIGURE 1 H-bond network of PYP in the active center.

timescales indicated here are only approximate and display a strong pH dependence (8,16,17). Central to the mechanism of photoactivation is the presence of a low-barrier H-bond between *p*CA and E46 in the ground state. Photoactivation causes a breakage of this low-barrier H-bond, followed by significant conformational rearrangement of all helices except part of helix α_5 (14). Thus, a distinct epitope is presented for interaction with downstream partners in the phototactic response, although the corresponding signaling pathway remains unknown (9).

To study the role of electrostatic interactions in protein function, it is important to assemble a set of NMR experiments that can accurately determine the protonation states of titratable amino acid side chains. One can determine individual pK_a values by following chemical shifts of nuclei in the amino acid side chain. The first, obvious choice is ^{1}H NMR (18), which because of its high NMR receptivity does not require any isotopic enrichment. However, there are several challenges to be overcome: the ^{1}H NMR spectrum of larger proteins is highly crowded, the response of ^{1}H chemical shifts to protonation state is often relatively small, and ^{1}H chemical shifts are sensitive to ionization equilibria other than that of the amino acid to which the proton is attached (18). The chemical shifts of ^{13}C or ^{15}N nuclei at the site of (de)protonation tend to undergo larger (>1 ppm) chemical-shift changes, and are therefore ideal reporters of protonation states. Moreover, such large variations in nuclear shielding are caused mainly by changes in the electron distribution within the side chain, rather than by charges that develop in the environment, and can therefore be used as more-selective probes of protonation states and the pK_a values of amino acid side chains.

To accurately determine the protonation states of Tyr residues, one can use several ^{13}C chemical shifts as reporters for the charge state of the Tyr ring, as shown in Table 1 and Fig. 2 (19).

1D ^{13}C NMR on uniformly ^{13}C-enriched protein samples is hindered by the presence of ^{13}C-^{13}C splittings in the spectrum and additional overlap with the $^{13}C_\zeta$ signals of arginines. Therefore, 1D ^{13}C NMR has been combined with

TABLE 1 ^{13}C chemical shift reporters in the Tyr side chain and their corresponding chemical shift changes upon deprotonation

Carbon chemical shift reporter	$\Delta\delta$ (ppm)
C_γ	−6.2
C_δ	0
C_ε	+3.3
C_ζ	+10.4

Values from Norton and Bradbury (19).

selective incorporation of ^{13}C-Tyr (20–22). In this approach, one obtains the assignments by removing individual Tyr residues through mutagenesis, which requires the parallel production and purification of multiple protein samples. Furthermore, one must ensure that the removal of each Tyr does not significantly perturb the structure, and thus the spectral change can be unambiguously attributed to the mutation site.

Alternatively, two-dimensional (2D) ^{1}H-^{13}C or ^{1}H-^{15}N NMR experiments applied to uniformly ^{13}C/^{15}N enriched proteins are ideally suited for recording the heteronuclear chemical shifts as a function of pH because they offer excellent sensitivity and resolution, and permit comprehensive and residue-specific assignments of individual amino acid resonances. So far, experiments of this type have been described for Asp, Glu, Lys, Arg, and His side chains, as well as the C- and N-termini (23–25), but an analogous method for addressing Tyr charge states was lacking until recently (26).

In this study, we present a strategy for comprehensively determining the pK_a values of the Tyr residues of PYP using indirect-detection 2D NMR spectroscopy of a uniformly

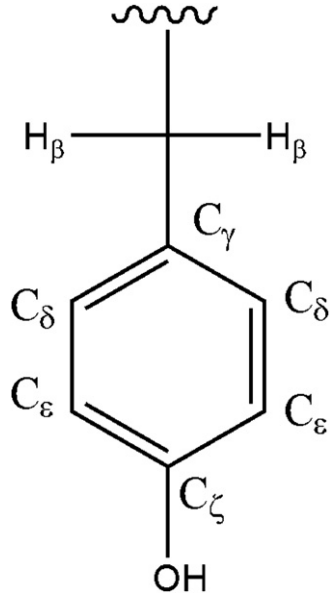

FIGURE 2 Tyrosine side chain.

^{13}C-enriched protein. We investigate the pH-dependent protonation state of Y42, which forms a short H-bond to the *p*CA chromophore, stabilizing its delocalized negative charge. The presence of a short H-bond under physiological conditions has been firmly established on the basis of x-ray and neutron crystallographic structures (6), NMR spectroscopic observation (14,7), and other spectroscopic data and theoretical calculations (27). However, the basis for the pH dependence of the photocycle kinetics is not fully understood at atomic resolution. Here, we show that Y42 remains fully protonated in the pH range of 3.41–11.24, indicating that the pH dependence of the PYP photocycle kinetics cannot be caused by changes in the charge state of Y42, and therefore it is very unlikely that the *p*CA chromophore undergoes changes in its electrostatic interactions in the electronic ground state.

MATERIAL AND METHODS

Sample preparation

Uniformly ^{13}C, ^{15}N-labeled wild-type PYP was produced in M9 minimal medium containing uniformly ^{13}C-enriched glucose and $^{15}NH_4Cl$ and purified as described previously (28). NMR samples contained ~1.0 mM of doubly labeled [^{13}C, ^{15}N] PYP, 0.15 mM DSS, 10% D_2O, and either 15 mM sodium acetate $-d_3$, 5 mM potassium phosphate, or 15 mM sodium bicarbonate as buffer for the pH ranges of 3.4–5.8, 5.9–8.6, and 8.7–11.24, respectively. The pH was changed in steps of 0.2 pH units by addition of a few microliters of concentrated HCl or NaOH solution.

To calibrate the pH meter (PB-11-P11; Sartorius Mechatronics, Nieuwegein, The Netherlands), we used standard calibration buffers of pH 4.0, 7.0, and 10.0. For measurements below pH 4 and above pH 10, we used a 0.1 M HCl solution (pH 1.0) and a 10 mM NaOH solution (pH 12) for calibration.

NMR spectroscopy

All NMR experiments were carried out on a Varian Unity INOVA 600 MHz spectrometer equipped with a pulsed field-gradient probe at 293 K. All aromatic proton-carbon correlations were established from 2D constant-time ^{1}H-^{13}C heteronuclear single quantum coherence (HSQC) spectra. This experiment was performed with the carrier position at 125 ppm in the ^{13}C domain. We recorded 512 (H^{aro}) × 128 (C^{aro}) complex points with maximum acquisition times of 64 and 16 ms for ^{1}H and ^{13}C, respectively. An interscan delay of 1 s was used with two scans per free induction decay (FID), giving rise to a measurement time of 9 min.

To obtain the signal from two-bond correlations between C_ζ and H_ε, we performed a constant-time ^{1}H-^{13}C HSQC experiment with the INEPT delay set to 24 ms (29). We recorded 512 (H^{aro}) × 128 (C^{aro}) complex points with maximum acquisition times of 64 and 16 ms for ^{1}H and ^{13}C, respectively. The number of scans per FID was 96, and the interscan delay was 1 s. The total experiment time was 7.5 h.

We recorded C_γ-H_β correlations in Tyr side chains using a 2D CG(CB)HB experiment with constant-time C_γ evolution (30). We acquired the spectra using 90 (C_γ) × 512 (H_β) complex points with maximum evolution times equal to 15 and 64 ms, respectively. The carrier position was placed at 130 ppm in the ^{13}C domain to excite the C_γ region. An interscan delay of 1 s was used, and 20 scans per FID were recorded, giving a total experiment time of ~1 h for every 2D spectrum.

We processed all of the spectra using NMRPipe (31) and analyzed them using SPARKY (32). Mirror-image linear prediction was applied during processing to extend the ^{13}C time-domain signal and improve the spectral resolution. All chemical shifts were referenced to DSS based on the IUPAC recommendation (33).

All Tyr peaks were assigned based on the strategy described by Oktaviani et al. (34). The complete assignment of PYP will be presented in a forthcoming publication.

Data analysis

The titration data for all Tyr chemical shifts were fitted to the Henderson-Hasselbalch equation, which is appropriate for rapid exchange of the nuclei between the environments associated with the neutral and charged states of the side chain:

$$\delta_{obs} = \delta_{AH} + \Delta\delta \frac{10^{n_H(pH-pK_a)}}{1 + 10^{n_H(pH-pK_a)}}, \quad (1)$$

where δ_{AH} denotes the chemical shift for the protonated form, $\Delta\delta = \delta_{A^-} - \delta_{AH}$ is the change in chemical shift upon deprotonation, and n_H is the Hill coefficient ($n_H > 1$ indicates apparent positive cooperativity). All calculations were performed with the use of Mathematica (Wolfram).

RESULTS AND DISCUSSION

Because the chemical-shift response to (de)protonation is sufficiently large for $^{13}C_\varepsilon$, in principal one could unambiguously determine the charge state of individual Tyr side chains by recording 2D HSQC or heteronuclear multiple-quantum correlation (HMQC) spectra, which exhibit high sensitivity. The 2D ^{1}H-^{13}C HSQC spectrum for PYP is shown in Fig. 3.

Signals for the surface-exposed residue Y98 are easily identified. Y76 overlaps with Y118, but resonances for Y42, Y94 are weak or invisible. This is probably due to the slow rotation of several tyrosines in the protein interior leading to exchange broadening. This may be a serious limitation for experiments that aim to use the H_δ or H_ε ring-proton resonances for other proteins as well.

Alternatively, 2D experiments that correlate ^{13}C with a ^{1}H nucleus two bonds removed via successive homonuclear and heteronuclear transfer through large one-bond couplings have been designed for the determination of acidic side-chain groups of Asp and Glu and the C-terminus (25). These experiments offer excellent sensitivity and resolution. In a recent study (26), a 2D HE(CE)CZ pulse sequence that correlates H_ε and C_ζ was successfully applied to determine the Tyr pK_a in *Bacillus circulans* xylanase. An approach to assign Tyr $^{13}C_\zeta$ in the context of SAIL isotope labeling (29) employs the two-bond H_ε-C_ζ coupling. This experiment is also applicable to uniformly enriched samples, where three-bond H_δ-C_γ correlations may also be observed. Unfortunately, these experiments suffer from sensitivity losses in the case of ring flips, when the H_δ and H_ε protons move between different magnetic environments. In the case of PYP, only signals from Y76 and Y98 are observed in the latter experiment, as shown in Fig. 4.

An alternative approach would be to indirectly detect $^{13}C_\gamma$ chemical shifts, which can be correlated to H_β

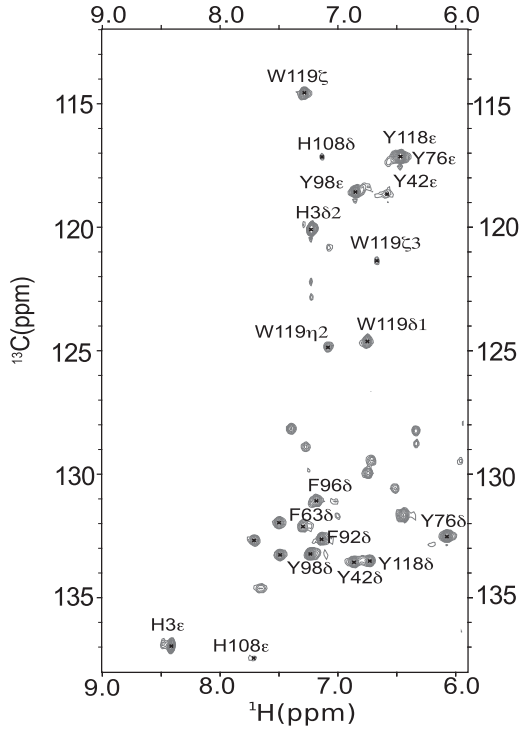

FIGURE 3 Region of the 2D aromatic ^{13}C-^{1}H HSQC spectrum for PYP containing the Tyr C-H correlations. The peak of Y118 C_ε overlaps with Y76 C_ε. Signals for Trp, and His side chains also fall in this spectral region. Assignments of the correlations are indicated.

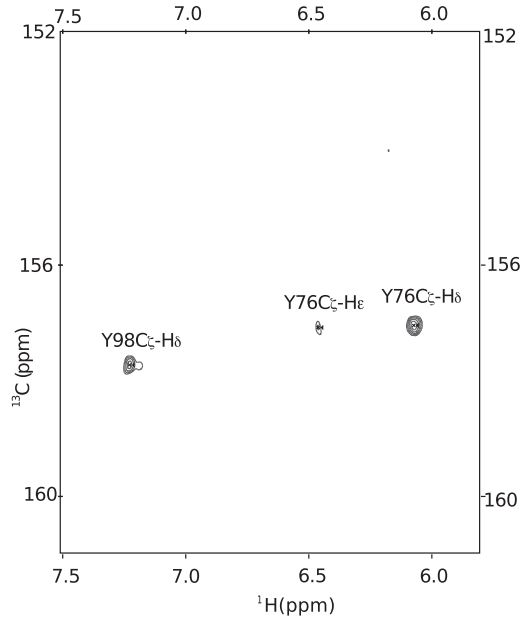

FIGURE 4 2D ^{13}C-^{1}H HSQC spectrum that correlates H_δ and H_ε with C_ζ for Tyr residues of PYP. Assignments of the correlations are indicated. Signals for Y42, Y94, and Y118 were not observed.

chemical shifts via successive magnetization transfers through the large $C_\gamma C_\beta$ ($^{1}J_{CC}$ ~45 Hz) and $C_\beta H_\beta$ ($^{1}J_{CH}$ ~130 Hz) coupling constants. This could be done via an out-and-back HB(CB)CG experiment, but for larger proteins, one could obtain increased sensitivity by avoiding one of the long and lossy homonuclear ^{13}C-magnetization transfer steps, by starting on the nonprotonated $^{13}C_\gamma$ (30). CG(CB)HB spectra are generally well resolved, even for larger proteins (>20 kDa), because they exhibit significant variation in the C_γ chemical shift as a function of amino acid type and secondary structure, and because there are two nonequivalent protons available to read out the C_γ shift in the resulting 2D spectrum. Partial deuteration will improve the sensitivity of the technique for proteins with higher molecular weights (35,36). Improved sensitivity of HB(CB)CG-type measurements has been achieved with a ~50% level of deuteration (37). For PYP, we observed all Tyr side-chain signals with good sensitivity, and there was not a single instance of overlap in the spectrum (Fig. 5). In addition, we were able to detect the C_γ resonance of H3 (which showed a pK_a value of 6.5) but not that of H118. We note that His C_γ detection could be improved by ^{15}N decoupling during C_γ evolution, which was not done here.

We followed the various chemical shifts that can be used as reporters of the side-chain charge state for the two Tyr residues that titrate below pH 11 (see Table 2). For Y76 and Y98, we can confirm that the chemical shifts of C_γ and C_ε stand out as responsive reporters for the side-chain protonation state, and that the C_δ resonance positions cannot be employed for this purpose. The small pH-dependent changes measured for the ring-proton chemical shifts yield pK_a values that are within 0.1 from those determined by ^{13}C chemical shifts. However, small changes in ^{1}H shifts can also result from changes in the charge states of nearby side chains. In particular, the pK_a values of Lys amino

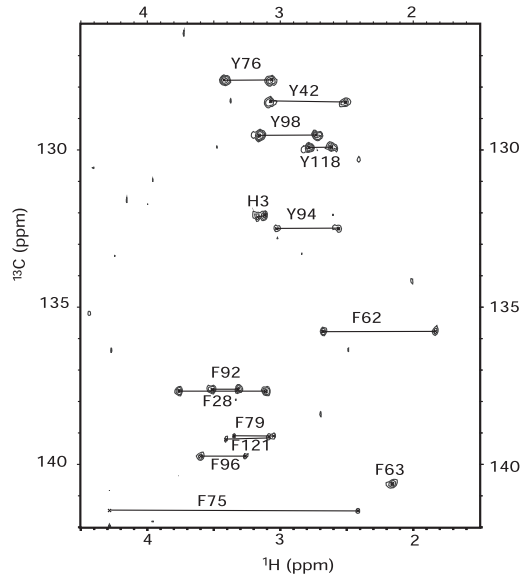

FIGURE 5 2D CG(CB)HB spectrum that correlates $H_{\beta 2}/H_{\beta 3}$ with C_γ for Tyr residues of PYP. His correlations were also detected. Assignments are indicated.

TABLE 2 Best-fit values for the pH-dependent ^{13}C chemical-shift changes and pK_a values of Y76 and Y98 of PYP

Residue	Nucleus*	δ_0 (ppm)	$\Delta\delta$ (ppm)	pK_a	n_H
Y76	C_δ	132.47	–	–	–
	C_ε	117.1 ± 0.1	2.23 ± 0.04	10.14 ± 0.02	1.24 ± 0.06
	C_γ (at $H_{\beta2/3}$)	127.8 ± 0.1	−3.77 ± 0.08	10.21 ± 0.02	1.16 ± 0.04
	H_β	3.003	–	–	–
	H_δ	6.05	–	–	–
	H_ε	6.46 ± 0.04	0.162 ± 0.004	10.1 ±0.03	1.3 ± 0.1
Global fit†	C_δ	132.47 ± 0.02	−0.08 ± 0.02		
	C_ε	117.1 ± 0.1	2.30 ± 0.04	10.20 ± 0.03	1.18 ± 0.06
	C_γ	127.7 ± 0.1	−3.73 ± 0.06		
Y98	C_δ	133.00	–	–	–
	C_ε	118.6 ± 0.1	2.8 ± 0.1	10.32 ± 0.03	1.12 ± 0.08
	C_γ (at $H_{\beta2/3}$)	129.5 ± 0.1	−4.8 ± 0.1	10.20 ± 0.01	1.54 ± 0.06
	H_β	3.15	–	–	–
	H_δ	7.231 ± 0.004	0.157 ± 0.04	10.43 ± 0.03	1.05 ± 0.05
	H_ε	6.85 ± 0.01	0.28 ± 0.01	10.37 ± 0.04	1.14 ± 0.1
Global fit†	C_δ	133.00 ± 0.02	−0.23 ± 0.02		
	C_ε	118.6 ± 0.1	2.5 ± 0.1	10.21 ± 0.03	1.48 ± 0.08
	C_γ	129.5 ± 0.1	−4.8 ± 0.1		

*C_δ, C_ε, H_δ, and H_ε resonances were monitored by ^{13}C-^{1}H HSQC spectroscopy; C_γ and H_β resonances were recorded by CG(CB)HB spectroscopy.
†For global fitting, the four titrations pertaining to the same Tyr ring (probed at $C_\gamma H_{\beta2}$, $C_\gamma H_{\beta3}$, $C_\delta H_\delta$, and $C_\varepsilon H_\varepsilon$) were combined and fitted simultaneously to a model with one pK_a and one n_H for that Tyr. Standard deviations (SDs) for the best-fit parameters resulting from the individual fits were estimated by analysis of the χ^2 function (43). For the global-fit parameters, the SDs were estimated via a Monte Carlo protocol in which estimated SDs per data point (0.05 in pH and 0.03 ppm in chemical shift) were used. See text for further discussion about the accuracy of these results.

groups are very similar to those of Tyr side chains, and this could lead to misinterpretation. The fact that this does not seem to occur for PYP is due to the spatial separation of the titrating groups. The fact that ^{1}H chemical shifts are particularly reactive to changes in the local distribution of charges is documented in the literature (38).

Fig. 6 *A* shows the location of the two solvent-exposed Tyr residues in PYP, together with titration curves of their $^{13}C_\gamma$ resonances. The pK_a values for the solvent-exposed residues Y76 and Y98 are 10.20 and 10.21, respectively, which is 0.5 units above the intrinsic pK_a reported for Tyr in aqueous solution (16). Because the net protein charge is approximately −6 at pH 9, this upshift of 0.5 units (which corresponds to an energy difference of ~2.8 kJ/mol) is probably due to coulombic forces that favor the neutral form of Tyr.

Fits of Eq. 1 to the experimental data improved significantly when the Hill parameters were allowed to become >1, especially for Y98. This is unusual for pH titrations in compactly folded proteins, where electrostatic interactions between nearby groups that titrate in the same pH range are expected to lead to an apparent negative cooperativity ($n_H < 1$). Even more puzzling is the observation that two titrations pertaining to the same residue (e.g,. Y98; see Table 2) yield different values for the Hill parameter. We conclude that small systematic errors (e.g., in the measurements of the highest pH values) must be part of the explanation. However, we also note that structural rearrangements in the direct environment of Tyr residues (in response to the increasing density of negative charges) can in principle explain the apparent positive cooperativity in their titration curves. The fact that the $^{13}C_\delta$ resonance shifts 0.23 ppm downfield in the pH range of ~10.5 (Table 2) is another indication that structural rearrangements must occur, because the $^{13}C_\delta$ chemical shift is normally unresponsive to ionization of the side chain (19).

As shown in Fig. 7 *A*, Y118 is partly (9%) buried within the protein interior, but its hydroxyl group is not involved in H-bonding. The titration curve for the $^{13}C_\gamma$ of Y118 is shown in Fig. 7 *B*. At the highest pH value, the $^{13}C_\gamma$ resonance has moved only −0.7 ppm. Assuming that $\Delta\delta = -4$ ppm (similar to the value measured for Y76), its estimated pK_a based on Eq. 1 is 11.6, which is higher than the values of the solvent-exposed residues Y76 and Y98. Substitution of $\Delta\delta$ values within the range of −3 to −6 ppm yielded estimated pK_a values between 11.4 and 12.0. The difference in the pK_a value of 1.4 pH units between solvent-exposed Tyr and buried Tyr can be explained by the different dielectric properties of water as a solvent and the protein interior, which is more hydrophobic (39). The more polar the environment, the more easily an acid/base can be ionized. Thus, in the hydrophobic environment of Y118, its pK_a has shifted to a higher value.

The two remaining Tyr residues in PYP, Y42 and Y94, are 82% and 27% buried, respectively, and involved in H-bonding. Their location in the protein is indicated in Fig. 8 *A*. Because the changes in their $^{13}C_\gamma$ chemical shifts are <0.1 ppm up to pH 11.24, the pK_a values of those side chains are significantly higher than 13 and cannot be determined reliably. The pK_a value of Y42 is of special mechanistic interest in the case of PYP, because this side chain shares a proton with the *p*CA chromophore, and forms a short H-bond. Our data demonstrate that this H-bond is

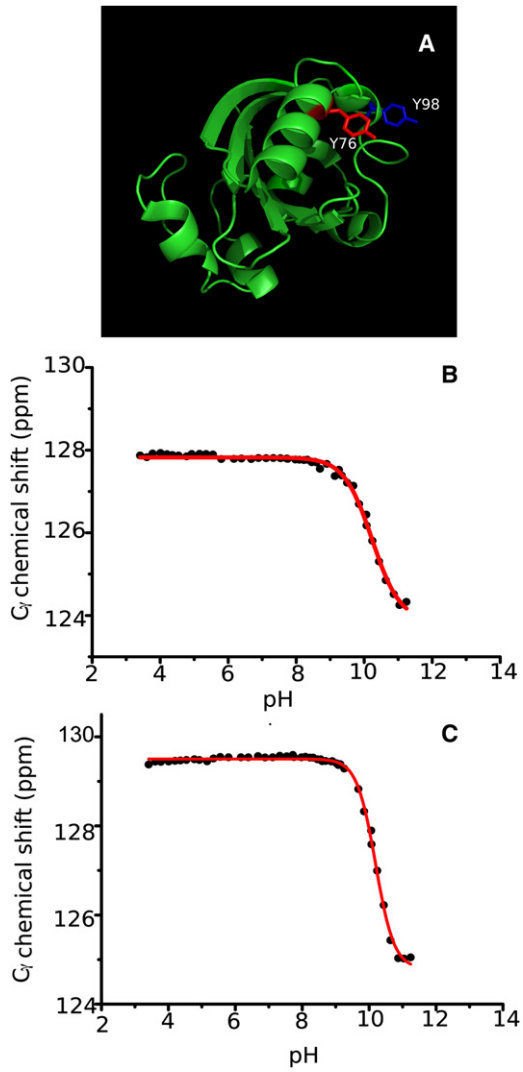

FIGURE 6 (*A*) PYP structure with the solvent-exposed residues Y76 and Y98 indicated. pH titration profile of Y76 (*B*) and Y98 (*C*) using the $^{13}C_\gamma$ chemical shifts as reporters.

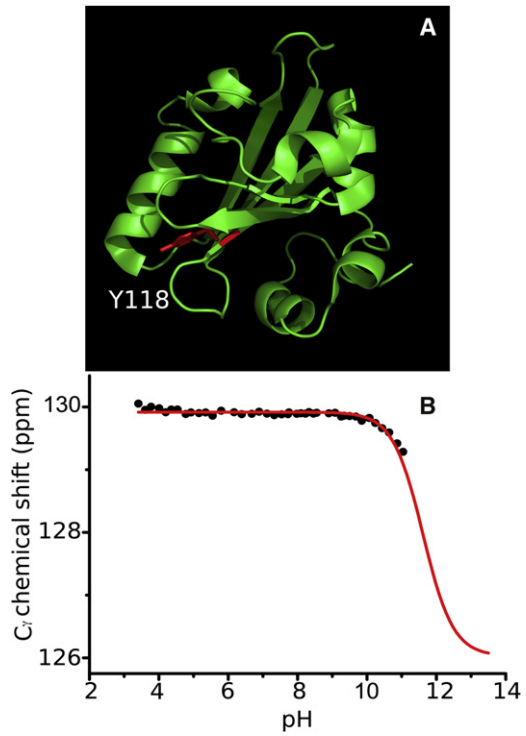

FIGURE 7 Buried Y118 in PYP structure (*A*) and its corresponding pH titration profile using the $^{13}C_\gamma$ chemical shift as reporter (*B*).

extremely stable and remains intact over the entire pH range, from 3.41 to 11.24 (see Fig. 8 *B*). In this pH range, the protein is folded and the active center is intact. However, the disruption of the H-bonding network involving the chromophore at very low pH (<3) results in partial protein unfolding (40), whereas at very high pH (>11) it leads to hydrolysis of the thioester bond that connects the *p*CA chromophore to C69 (41). Y42 is also known to play an important role in stabilizing the native conformation of the *p*CA chromophore through H-bonding. The mutation of Y42 into Phe (Y42F) disrupts the H-bond network between Y42 and the *p*CA chromophore, as well as that between Y42 and the hydroxyl group of T50. This causes the distance between F42 and T50 to increase due to van der Waals repulsion, and movement of the *p*CA chromophore toward T50. As a consequence, a second conformation of the *p*CA chromophore can be observed in the protein population as a shoulder in the UV/Vis spectrum at 391 nm (8). However, the Y42F mutation does not have a significant effect on the pH dependence of the photocycle kinetics. The maximum rate constant for the transition of pR to pB in the Y42F mutant occurs at a similar pH compared with wild-type PYP (8). This finding agrees with our result that Y42 remains fully protonated in the pH range of 3.41–11.24, which makes it unlikely that pH-induced changes observed in the photocycle kinetics of PYP are caused by changes in the electrostatic interactions involving the chromophore in the ground state.

Y94 is also buried and donates an H-bond to the backbone of C69 and the hydroxyl side chain of S72. Fig. 8 *B* shows that the protonation state of Y94 is pH-independent, indicating that Y94 is protonated over the entire pH range of 3.41–11.24. Although there is no direct H-bond between Y94 and the *p*CA chromophore, the stability of the H-bond network over a wide pH range may also be important for the stability of the thioester bond between C69 and *p*CA. This result is supported by the fact that the mutation Y94A shifts the absorption maximum by 4 nm toward the blue (442 nm) (42). In agreement with these findings, spectroscopic studies also imply that the H-bond between the side chain of Y94 and the hydroxyl side chain of S72 is important for maintaining the helical secondary structure (42).

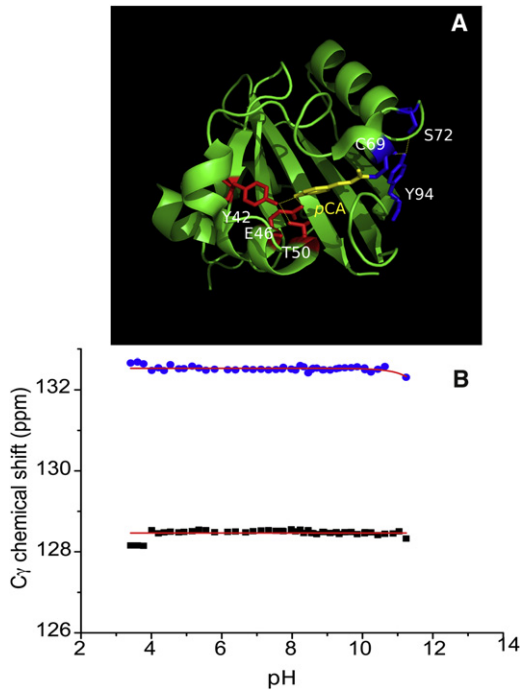

FIGURE 8 H-bonded Tyr side chains in PYP. (*A*) Y42 forms an H-bond to *p*CA and the hydroxyl group of T50, whereas Y94 forms H-bonds to the backbone of C69 and the hydroxyl group of S72. (*B*) pH titration profile of Y42 (*squares*) and Y94 (*circles*) using the $^{13}C_\gamma$ chemical shift as reporter.

CONCLUSIONS

We have presented an NMR approach based on 2D C_γ-H_β correlation spectroscopy to determine the residue-specific pK_a values of individual Tyr side chains in native proteins with high sensitivity and resolution. This approach offers a number of advantages over existing practices. Our approach does not require mutagenesis to assign the NMR resonances, and facilitates complete and comprehensive analyses of electrostatic interactions involving Tyr side chains in proteins.

For PYP from *H. halophila*, we were able to determine the pH dependence of the protonation states of all individual Tyr side chains. In PYP we observe three classes of tyrosines based on their titration behavior: solvent-exposed (Y76 and Y98), buried in the hydrophobic environment (Y118), and H-bonded (Y42 and Y94), with pK_a values of ~10, 12, and above 13, respectively. Our study also shows that the short H-bonds to the *p*CA chromophore persist over the entire pH range in which the protein is chemically and thermodynamically stable. Our data indicate that previous observations of pH-dependent changes in PYP photocycle kinetics cannot be caused by changes in the charge state of Y42, and it is therefore very unlikely that the *p*CA chromophore undergoes changes in its electrostatic interactions in the electronic ground state.

This work was supported by a VIDI career development award to F.A.A.M. from the Netherlands Organization for Scientific Research.

REFERENCES

1. Sprenger, W. W., W. D. Hoff, …, K. J. Hellingwerf. 1993. The eubacterium *Ectothiorhodospira halophila* is negatively phototactic, with a wavelength dependence that fits the absorption spectrum of the photoactive yellow protein. *J. Bacteriol.* 175:3096–3104.
2. Pellequer, J. L., K. A. Wager-Smith, …, E. D. Getzoff. 1998. Photoactive yellow protein: a structural prototype for the three-dimensional fold of the PAS domain superfamily. *Proc. Natl. Acad. Sci. USA.* 95:5884–5890.
3. Borgstahl, G. E., D. R. Williams, and E. D. Getzoff. 1995. 1.4 A structure of photoactive yellow protein, a cytosolic photoreceptor: unusual fold, active site, and chromophore. *Biochemistry.* 34:6278–6287.
4. Anderson, S., S. Crosson, and K. Moffat. 2004. Short hydrogen bonds in photoactive yellow protein. *Acta Crystallogr. D Biol. Crystallogr.* 60:1008–1016.
5. Fisher, S. Z., S. Anderson, …, A. J. Schultz. 2007. Neutron and X-ray structural studies of short hydrogen bonds in photoactive yellow protein (PYP). *Acta Crystallogr. D Biol. Crystallogr.* 63:1178–1184.
6. Yamaguchi, S., H. Kamikubo, …, M. Kataoka. 2009. Low-barrier hydrogen bond in photoactive yellow protein. *Proc. Natl. Acad. Sci. USA.* 106:440–444.
7. Sigala, P. A., M. A. Tsuchida, and D. Herschlag. 2009. Hydrogen bond dynamics in the active site of photoactive yellow protein. *Proc. Natl. Acad. Sci. USA.* 106:9232–9237.
8. Brudler, R., T. E. Meyer, …, E. D. Getzoff. 2000. Coupling of hydrogen bonding to chromophore conformation and function in photoactive yellow protein. *Biochemistry.* 39:13478–13486.
9. Imamoto, Y., and M. Kataoka. 2007. Structure and photoreaction of photoactive yellow protein, a structural prototype of the PAS domain superfamily. *Photochem. Photobiol.* 83:40–49.
10. Imamoto, Y., K. Mihara, …, K. Yoshihara. 1997. Evidence for proton transfer from Glu-46 to the chromophore during the photocycle of photoactive yellow protein. *J. Biol. Chem.* 272:12905–12908.
11. Xie, A., W. D. Hoff, …, K. J. Hellingwerf. 1996. Glu46 donates a proton to the 4-hydroxycinnamate anion chromophore during the photocycle of photoactive yellow protein. *Biochemistry.* 35:14671–14678.
12. Carroll, E. C., S. H. Song, …, D. S. Larsen. 2010. Subpicosecond excited-state proton transfer preceding isomerization during the photorecovery of photoactive yellow protein. *J Phys Chem Lett.* 1:2793–2799.
13. Ujj, L., S. Devanathan, …, G. H. Atkinson. 1998. New photocycle intermediates in the photoactive yellow protein from *Ectothiorhodospira halophila*: picosecond transient absorption spectroscopy. *Biophys. J.* 75:406–412.
14. Düx, P., G. Rubinstenn, …, R. Kaptein. 1998. Solution structure and backbone dynamics of the photoactive yellow protein. *Biochemistry.* 37:12689–12699.
15. van der Horst, M. A., I. H. van Stokkum, …, K. J. Hellingwerf. 2001. The role of the N-terminal domain of photoactive yellow protein in the transient partial unfolding during signalling state formation. *FEBS Lett.* 497:26–30.
16. Hendriks, J., and K. J. Hellingwerf. 2009. pH Dependence of the photoactive yellow protein photocycle recovery reaction reveals a new late photocycle intermediate with a deprotonated chromophore. *J. Biol. Chem.* 284:5277–5288.
17. Imamoto, Y., M. Harigai, and M. Kataoka. 2004. Direct observation of the pH-dependent equilibrium between L-like and M intermediates of photoactive yellow protein. *FEBS Lett.* 577:75–80.
18. Karplus, S., G. H. Snyder, and B. D. Sykes. 1973. A nuclear magnetic resonance study of bovine pancreatic trypsin inhibitor. Tyrosine titrations and backbone NH groups. *Biochemistry.* 12:1323–1329.
19. Norton, R., and J. Bradbury. 1974. Carbon-13 nuclear magnetic resonance study of tyrosine titrations. *J. Chem. Soc. Chem. Commun.* 21:870–871.

20. Kato-Toma, Y., T. Iwashita, …, M. Ishiguro. 2003. pK_a measurements from nuclear magnetic resonance of tyrosine-150 in class C β-lactamase. *Biochem. J.* 371:175–181.

21. Ugurbil, K., and R. Bersohn. 1977. Tyrosine emission in the tryptophanless azurin from *Pseudomonas fluorescens*. *Biochemistry.* 16: 895–901.

22. Wilbur, D. J., and A. Allerhand. 1976. Titration behavior of individual tyrosine residues of myoglobins from sperm whale, horse, and red kangaroo. *J. Biol. Chem.* 251:5187–5194.

23. André, I., S. Linse, and F. A. A. Mulder. 2007. Residue-specific pK_a determination of lysine and arginine side chains by indirect ^{15}N and ^{13}C NMR spectroscopy: application to apo calmodulin. *J. Am. Chem. Soc.* 129:15805–15813.

24. Hass, M. A., A. Yilmaz, …, J. J. Led. 2009. Histidine side-chain dynamics and protonation monitored by ^{13}C CPMG NMR relaxation dispersion. *J. Biomol. NMR.* 44:225–233.

25. Oda, Y., T. Yamazaki, …, H. Nakamura. 1994. Individual ionization constants of all the carboxyl groups in ribonuclease HI from *Escherichia coli* determined by NMR. *Biochemistry.* 33:5275–5284.

26. Baturin, S. J., M. Okon, and L. P. McIntosh. 2011. Structure, dynamics, and ionization equilibria of the tyrosine residues in *Bacillus circulans* xylanase. *J. Biomol. NMR.* 51:379–394.

27. Boggio-Pasqua, M., M. A. Robb, and G. Groenhof. 2009. Hydrogen bonding controls excited-state decay of the photoactive yellow protein chromophore. *J. Am. Chem. Soc.* 131:13580–13581.

28. Mihara, K., O. Hisatomi, …, F. Tokunaga. 1997. Functional expression and site-directed mutagenesis of photoactive yellow protein. *J. Biochem.* 121:876–880.

29. Takeda, M., J. Jee, …, M. Kainosho. 2009. Hydrogen exchange rate of tyrosine hydroxyl groups in proteins as studied by the deuterium isotope effect on C(ζ) chemical shifts. *J. Am. Chem. Soc.* 131: 18556–18562.

30. Prompers, J. J., A. Groenewegen, …, H. A. M. Pepermans. 1998. Two-dimensional NMR experiments for the assignment of aromatic side chains in ^{13}C-labeled proteins. *J. Magn. Reson.* 130:68–75.

31. Delaglio, F., S. Grzesiek, …, A. Bax. 1995. NMRPipe: a multidimensional spectral processing system based on UNIX pipes. *J. Biomol. NMR.* 6:277–293.

32. Goddard, T., and D. Kneller. 2004. SPARKY 3. University of California, San Francisco.

33. Markley, J. L., A. Bax, …, K. Wüthrich. 1998. Recommendations for the presentation of NMR structures of proteins and nucleic acids—IUPAC-IUBMB-IUPAB Inter-Union Task Group on the standardization of data bases of protein and nucleic acid structures determined by NMR spectroscopy. *Eur. J. Biochem.* 256:1–15.

34. Oktaviani, N. A., R. Otten, …, F. A. A. Mulder. 2011. 100% complete assignment of non-labile (1)H, (13)C, and (15)N signals for calcium-loaded Calbindin D(9k) P43G. *Biomol. NMR Assign.* 5:79–84.

35. Constantine, K. L., L. Mueller, …, B. T. Farmer, 2nd. 1997. Characterization of NADP+ binding to perdeuterated MurB: backbone atom NMR assignments and chemical-shift changes. *J. Mol. Biol.* 267: 1223–1246.

36. Gardner, K. H., and L. E. Kay. 1998. The use of ^{2}H, ^{13}C, ^{15}N multidimensional NMR to study the structure and dynamics of proteins. *Annu. Rev. Biophys. Biomol. Struct.* 27:357–406.

37. Paquin, R., F. Ferrage, …, G. Bodenhausen. 2008. Multiple-timescale dynamics of side-chain carboxyl and carbonyl groups in proteins by ^{13}C nuclear spin relaxation. *J. Am. Chem. Soc.* 130:15805–15807.

38. Webb, H., B. M. Tynan-Connolly, …, J. E. Nielsen. 2011. Remeasuring HEWL pK(a) values by NMR spectroscopy: methods, analysis, accuracy, and implications for theoretical pK(a) calculations. *Proteins.* 79:685–702.

39. Harris, T. K., and G. J. Turner. 2002. Structural basis of perturbed pK_a values of catalytic groups in enzyme active sites. *IUBMB Life.* 53:85–98.

40. Craven, C. J., N. M. Derix, …, R. Kaptein. 2000. Probing the nature of the blue-shifted intermediate of photoactive yellow protein in solution by NMR: hydrogen-deuterium exchange data and pH studies. *Biochemistry.* 39:14392–14399.

41. Hoff, W. D., B. Devreese, …, K. J. Hellingwerf. 1996. Chemical reactivity and spectroscopy of the thiol ester-linked *p*-coumaric acid chromophore in the photoactive yellow protein from *Ectothiorhodospira halophila*. *Biochemistry.* 35:1274–1281.

42. Morishita, T., M. Harigai, …, Y. Imamoto. 2007. Array of aromatic amino acid side chains located near the chromophore of photoactive yellow protein. *Photochem. Photobiol.* 83:280–285.

43. Berendsen, H. J. C. 2011. A student's guide to data and error analysis. Cambridge University Press, Cambridge, UK.